

Magnetic-field-induced recovery of resonant tunneling into a disordered quantum well subbandF. Pulizzi,^{1,*} E. E. Vdovin,^{2,1} K. Takehana,^{1,†} Yu. V. Dubrovskii,^{2,1} A. Patané,¹ L. Eaves,¹ M. Henini,¹ P. N. Brunkov,^{3,1} and G. Hill⁴¹*School of Physics and Astronomy, University of Nottingham, University Park, Nottingham NG7 2RD, United Kingdom*²*Institute of Microelectronics Technology RAS, 142432 Chernogolovka, Russia*³*A. F. Ioffe Physico-Technical Institute, Polytechnicheskaya 26, 194021 St. Petersburg, Russia*⁴*Department of Electronic and Electrical Engineering, University of Sheffield, Sheffield S3 3JD, United Kingdom*

(Received 28 April 2003; revised manuscript received 24 July 2003; published 20 October 2003)

We investigate how the disorder produced by a layer of self-assembled InAs quantum dots affects the electronic states of a GaAs quantum well incorporated in a double barrier resonant tunneling diode. The disorder strongly suppresses the resonant peak in the current due to electron tunneling into the lowest energy subband of the quantum well. However, the peak is recovered by the application of an in-plane magnetic field, which provides a means of tuning the in-plane momentum of the tunneling electrons. Analysis of these data and of Landau level formation when the field is applied perpendicular to the quantum well plane provides information about the length-scale of disorder potential in the well.

DOI: 10.1103/PhysRevB.68.155315

PACS number(s): 73.23.-b, 73.63.Kv, 73.40.Gk

Self-assembled semiconductor quantum dots (QD's) produced by the Stranskii-Krastanov growth mode are of fundamental interest and have great potential for novel optoelectronic devices.¹ QD's have been incorporated in a wide range of semiconductor structures. Several groups have investigated devices in which a layer of QD's is placed in close proximity to a modulation-doped two-dimensional electron gas (2DEG).²⁻⁵ The dots act as a store of electron charge and create a controllable disordered potential, which modifies the conductivity and the electron mobility of the 2DEG. The dots were either incorporated in a single (AlGa)As tunnel barrier^{6,7} or else in, or close to, a GaAs quantum well surrounded by two (AlGa)As barriers.^{8,9} Tunneling spectroscopy has been used in this type of structures to study transport through the highly localized zero-dimensional electronic states of a dot.⁸ Devices of this type show promise for memory and single photon applications.¹⁰⁻¹² However, to date little information exists about the extended states of a GaAs quantum well (QW) incorporating a layer of QD's, a heterostructure design that has been employed for a number of device applications, such as QD lasers.^{13,14}

In this paper we use resonant magnetotunneling to investigate the effect of the disordered potential produced by a layer of QD's on electrons tunneling through a QW, which is incorporated in a double barrier resonant tunneling diode (RTD). By measuring the tunnel current as a function of the bias voltage and of magnetic field B_{\parallel} applied parallel to the plane of the QW, we can study the effect of disorder on the electronic states of the QW subband over a wide range of energy (ϵ) and in-plane momentum (k_{\parallel}). In the absence of disorder, both the electron energy and the in-plane component of the electron momentum are conserved when an electron tunnels through a barrier. As a result, resonant peaks are observed in the current-voltage characteristic $I(V)$ of the RTD. Due to the steplike character of the density of states of a QW, the momentum conservation condition is essential for observing a peak and the associated negative differential conductivity (NDC) in the $I(V)$ curves. The destruction of translational symmetry due to the presence of disorder in the

QW breaks the momentum conservation condition and tends to smear out the peak in $I(V)$. We find that a layer of QD's in the center of the QW produces sufficient disorder to destroy the resonance associated with the lowest energy subband of the QW. However, the resonant peak and the NDC associated with the lowest QW subband are restored by the application of a sufficiently strong in-plane magnetic field. We explain this behavior in terms of the effect of the magnetic field and applied bias on the dynamics of electron tunneling into the states of the disordered QW. In addition, we study the effect of the QD's on the formation of Landau levels in the QW. By measuring the dependence of the current on a magnetic field B_{\perp} applied perpendicular to the QW plane, we show that Landau levels form when the cyclotron orbits extend over lengths smaller than the average spatial separation between the QD's.

The technique used in our experiment, termed magnetotunneling spectroscopy (MTS), has been previously used to study the electronic properties of a number of different semiconductor heterostructure systems including donors in QW's,¹⁵ quantum wires,¹⁶ and quantum dots.^{8,9,17} It has also helped to identify many of the interesting features, e.g., negative hole effective mass, anisotropy, and band-mixing effects, predicted theoretically for valence^{18,19} and conduction band QW's.²⁰ Here we show that MTS can provide us with a useful means of probing the electronic states of a strongly disordered QW, in which the dots act as the source of disorder.

The device used in our experiment is a double barrier electron RTD grown by molecular beam epitaxy (MBE) on a (100)-oriented n^+ GaAs substrate. A layer of InAs QD's was embedded in the center of a 12-nm GaAs QW, sandwiched between two 8.3-nm $\text{Al}_{0.4}\text{Ga}_{0.6}\text{As}$ tunnel barriers, as shown schematically in Fig. 1(a). The QD's were grown by depositing 2.3 InAs monolayers (ML's) on a 6-nm GaAs layer, annealing for 90 sec at 620 °C, and then capping with a second 6-nm GaAs layer to complete the QW. On each side of the two $\text{Al}_{0.4}\text{Ga}_{0.6}\text{As}$ barriers the layer structure is as follows: a 50-nm GaAs undoped spacer layer, a 50-nm GaAs

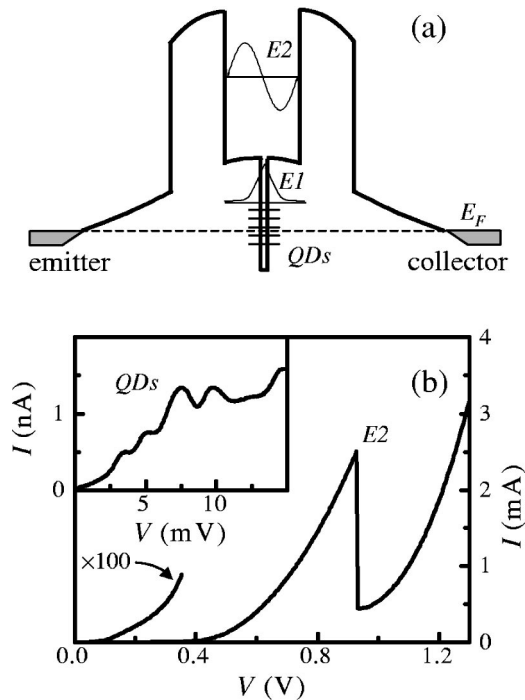


FIG. 1. (a) Schematic conduction-band profile of a double barrier resonant tunneling diode (RTD) incorporating InAs QD's in the center of a GaAs/Al_{0.4}Ga_{0.6}As QW. (b) $I(V)$ characteristic at zero magnetic field. Inset: $I(V)$ at low bias, showing peaks due to tunneling through localized states of the QD's.

layer n doped to $2 \times 10^{17} \text{ cm}^{-3}$, and $0.4\text{-}\mu\text{m}$ GaAs layers n^+ doped to $3 \times 10^{18} \text{ cm}^{-3}$, which form the outer electrical contacts of the device. Atomic force microscopy images of a structure with QD's grown under the same conditions reveal a distribution of dot sizes consisting of two components: small dots of typical in-plane diameter $d \sim 50 \text{ nm}$ and density $\rho \sim 10^{10} \text{ cm}^{-2}$, and larger anisotropic dots with typical in-plane sizes of 70 and 250 nm, and density $\rho \sim 2.0 \times 10^9 \text{ cm}^{-2}$.²¹

The confinement in the growth direction generates two two-dimensional electronic subbands $E1$ and $E2$, in which the electrons are free to move in the QW plane. Figure 1(a) shows schematically how the presence of the InAs layer affects the conduction band profile and energy levels in the QW. The states of the lowest energy subband $E1$, for which the wave function has a maximum in the center of the QW, are shifted markedly to lower energy. A simple quantum calculation indicates that the $E1$ subband moves below the conduction band edge of GaAs in the QW. In the limit of a very wide QW, the $E1$ subband would correspond to the InAs wetting layer level that forms beneath the QD's. In contrast, the energy of the $E2$ subband, for which the wave function as a node near the QD layer, has an energy similar to that in a control sample in which the QD layer is absent. At zero bias, equilibrium is established by charging of the QD's due to diffusion of electrons from the doped contact layers.²² This leads to the electrostatic band bending effect shown schematically in Fig. 1(a), which raises the energy of all states in the quantum well, including $E1$, relative to the

Fermi energy in the emitter. Hence, this subband should come into resonance with the emitter Fermi energy when a bias is applied, thus producing a resonant peak in the $I(V)$. However, as discussed in detail below, this resonant peak is not observed at $B_{\parallel} = 0$.

As shown in Fig. 1(b), the low temperature ($T = 4.2 \text{ K}$) $I(V)$ characteristic at zero magnetic field reveals a clear peak ($E2$) at a bias voltage of 0.95 V due to electron tunneling into the second electron subband of the QW. The resonant peak associated with electron tunneling into the first QW subband ($E1$) is absent, whereas it is observed, around 0.2 V, in control samples with similar layer composition except that the QD layer is absent.²² For the sample containing QD's, the current increases with bias showing a change in the slope of the $I(V)$ at biases smaller than 0.4 V. This is attributed to the formation of an electron accumulation layer adjacent to the first barrier. Also, at very low bias ($\leq 0.1 \text{ V}$), we observe additional resonant features, due to tunneling of electrons into the QD states [inset of Fig. 1(b)]. These modulation of current also reflects fluctuations of the density of states in the emitter.²³

Figure 2(a) shows that a clear and well-defined resonant peak in $I(V)$ at a bias of $\sim 0.2 \text{ V}$ appears when a strong magnetic field ($B_{\parallel} \geq 5 \text{ T}$) is applied parallel to the plane of the QW. By further increasing the magnetic field to 6.5 T, the $I(V)$ shows NDC. The two steps present in the region where we observe NDC (indicated by the stars for the $B_{\parallel} = 11 \text{ T}$ curve) are associated with high frequency oscillations in the current, which can be suppressed by placing a capacitor across the device or by decreasing the lateral size of the device [as shown in the inset of Fig. 2(b)]. Figure 2(b) shows the $I(V)$ curves for B_{\parallel} up to 12 T. The emergence of the resonance is shown in the differential conductance ($G = dI/dV$) greyscale plot depicted in Fig. 2(c). With increasing B_{\parallel} , the resonance shifts to higher bias with a parabolic trend [white line in Fig. 2(b)], and both the resonance width and magnitude of the current increase. The parabolic dependence strongly suggests that the resonance is due to electron tunneling into the extended states of an energy band,²⁴ which we ascribe to the lowest QW subband $E1$. In contrast, for tunneling into the localized states of quantum dots, the applied magnetic field has very little effect on the peak position of the resonant peaks, while the amplitude of the peaks decreases strongly.^{8,9}

The emergence of the $E1$ resonance with increasing in-plane magnetic field indicates that the disorder has a decreasing effect on the tunneling electrons. The disorder arises partly from electron charging of some of the dots and partly from the morphological and strain disorder of the InAs layer. Let us assume that the disordered potential in the QW plane is spatially modulated over a characteristic length scale l_d . For $B_{\parallel} = 0$, electrons tunnel into the QW with in-plane kinetic energy $\epsilon_{\parallel} = \hbar^2 k_{\parallel}^2 / 2m^*$, where k_{\parallel} is the electron in-plane k vector and m^* is the electron effective mass. For $k_{\parallel} \leq k_d$, where $k_d = 2\pi/l_d$, the electron is strongly scattered by the disorder. As a result, at low ϵ_{\parallel} , the in-plane momentum is not conserved in the tunneling process and the expected resonant peak is smeared out to give a broadened steplike feature in $I(V)$. This smearing effect is particularly pronounced for

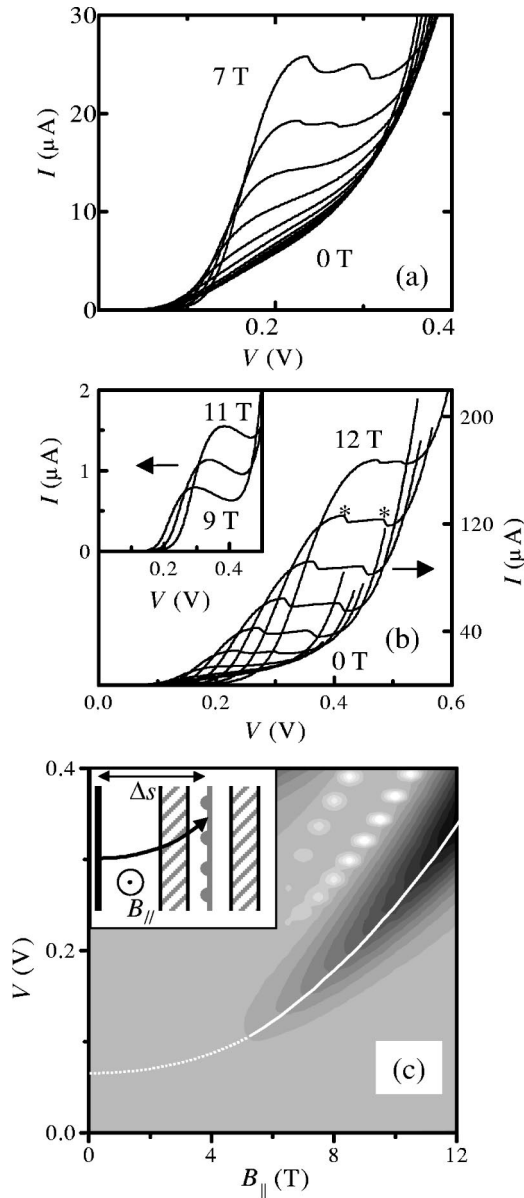


FIG. 2. (a) $I(V)$ curves for $B_{\parallel} \leq 7$ T (every 0.5 T) to make evident the emergence of a resonance at $B_{\parallel} = 5$ T measured on a mesa with 400 μm diameter. (b) $I(V)$ curves for B_{\parallel} in the range 0 to 12 T. The inset shows $I(V)$ curves measured on a mesa with 50 μm diameter, where the two steps in the NDC region observed in the larger mesa (see text) are not present. (c) Greyscale plot of the differential conductance as a function of V and B_{\parallel} . The maximum of the conductance is represented by the black color. The white color represents negative differential conductance. The white solid line shows the parabolic increase of the voltage position of the resonance peak. The series of white dots in the greyscale plot of $G(V)$ observed for $B_{\parallel} > 5$ T and $V > 0.2$ V comes from the sharp downward steps in $I(V)$ in the NDC region and from the finite step in B_{\parallel} (0.5 T). Inset: sketch of the deflection of the electron trajectory in the presence of B_{\parallel} .

electrons tunneling into the lowest energy subband $E1$, which has an antinode in its wave function close to the position of the QD layer [see Fig. 1(a)]. In contrast, the upper QW subband $E2$ has a node in its wave function close to the

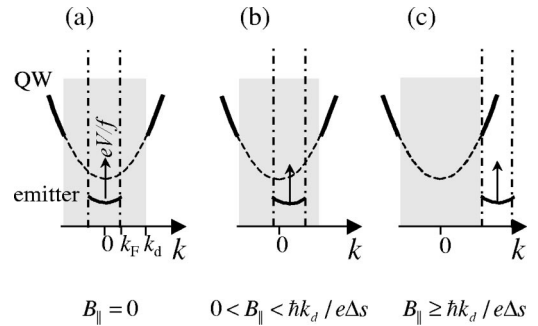


FIG. 3. Schematic representation of the effect of an in-plane magnetic field B_{\parallel} and bias V on the tunneling of electrons from the emitter to the QW subband states. B_{\parallel} provides the tunneling electrons with an in-plane momentum component $\Delta k = eB_{\parallel}\Delta s/\hbar$. The application of V provides the electrons in the emitter with an extra energy eV/f .

QD's. Hence the effect of disorder is much weaker for electrons tunneling into this subband with the result that electron tunneling into $E2$ produces a clear and intense peak in the $I(V)$ curve [see Fig. 1(b)].

Figure 3 illustrates the mechanism that we propose to explain the magnetic field-induced emergence of resonance $E1$. As outlined above, for $k < k_d$ the in-plane momentum is not conserved in the tunneling process because of disorder. We represent this effect in Fig. 3(a) by showing the energy dispersion band of the QW at low k_{\parallel} values by a dashed line. In terms of this model, the resonant peak expected in $I(V)$ when the bias brings the emitter energy in alignment with the QW band is smeared out by the disorder. An in-plane magnetic field causes an electron tunneling into the $E1$ subband to acquire an additional in-plane momentum component $\Delta k = eB_{\parallel}\Delta s/\hbar$, due to the action of the Lorentz force [see Figs. 2(c), 3(b), 3(c)].^{19,25} Here Δs (~ 26 nm) is the effective tunneling length between the quasibound electron state in the accumulation layer and the center of the QW. The resonant condition is restored at magnetic fields large enough to supply the momentum $\hbar\Delta k \geq \hbar k_d$ [Fig. 3(c)].

As can be seen from Fig. 2(a), the $E1$ feature emerges as a clear resonance in $I(V)$ at a field of about 5 T, corresponding to $\Delta k \approx 2 \times 10^8 \text{ m}^{-1}$. Above 5 T, the bias position of the resonance shifts parabolically with B_{\parallel} , according to the relation $e\Delta V = f\hbar^2\Delta k^2/2m^*$. Here f is the electrostatic leverage factor ($f=5$), which determines the fraction of the total applied bias dropped across Δs , $m^* = 0.067m_0$, where m_0 is the electron mass in vacuum and ΔV is the variation of the voltage position of the resonance relative to its value at zero magnetic field. This indicates that electrons tunnel resonantly with both energy and momentum conservation into states of the parabolic $E1$ subband with $k_{\parallel} \geq k_d \approx 2 \times 10^8 \text{ m}^{-1}$. The $E1$ resonance is smeared out at low bias and low magnetic field by potential fluctuations with a characteristic length scale $l_d = 2\pi/k_d \approx 30$ nm, which compares with the typical size and separation of the higher density QD's present in our sample. Further investigation with different orientations of B_{\parallel} in the QW plane, aimed to search for any anisotropy of the disorder potential, show no dependence of the $I(V)$ curves on the orientation of B_{\parallel} . This suggests that the effects

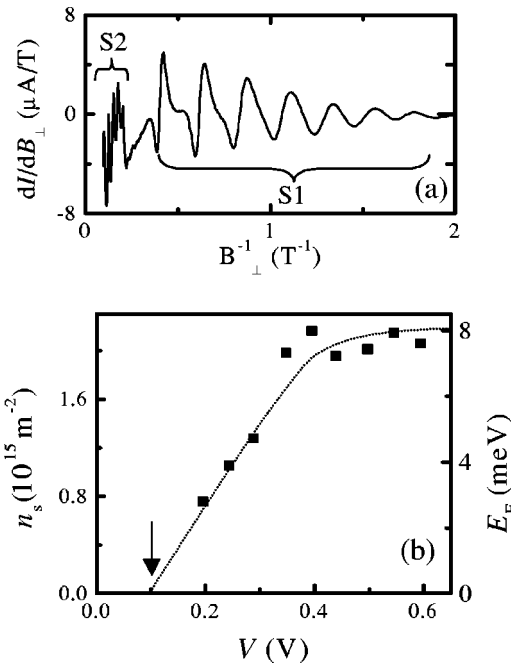


FIG. 4. (a) dI/dB_{\perp} vs B_{\perp}^{-1} at a bias voltage of 0.5 V. S1 and S2 indicate two different series of magneto-oscillations. (b) Voltage dependence of the electron density n_s and Fermi energy E_F in the emitter layer. The dotted line is a guide for the eye. The arrow indicates the voltage at which the emitter accumulation layer forms.

observed in the tunneling current are due to the disorder induced by the smaller dots and not by the strongly anisotropic low density QD's.

The disorder due to the QD's also affects the Landau levels in the QW that form when a magnetic field B_{\perp} is applied perpendicular to the QW plane. We have measured the $I(B_{\perp})$ curves for several values of applied bias. For $V > 0.2$ V, we observe two distinct series of Shubnikov-de Haas-like oscillations, both periodic in inverse magnetic field B_{\perp}^{-1} . Figure 4(a) shows the derivative of the $I(B_{\perp})$ curve for $V = 0.5$ V. The series S1 is related to the Landau levels in the two-dimensional emitter accumulation layer. The oscillations in the current arise from the passage of the Landau levels through the accumulation layer Fermi energy as B_{\perp} is increased. From the period of the oscillations B_{\perp}^{-1} , and using the relation $n_s = 2eB_{\perp}f/h$, we calculate the electron sheet density n_s in the accumulation layer [see Fig. 4(b)]. This

analysis shows that a two-dimensional accumulation layer starts to form at $V \approx 0.1$ V [see arrow in Fig. 4(b)].

The higher frequency series (S2) arises from scattering-assisted electron tunneling from the emitter into discrete Landau levels of the EI QW subband accompanied by a change of the Landau level index.²⁶ We can estimate the diameter of the cyclotron orbit associated with a Landau level using the relation

$$d_c = 2l_B \sqrt{2p+1}, \quad (1)$$

where $l_B = \sqrt{\hbar/eB_{\perp}}$ is the magnetic length and p is the Landau level index. We find that the largest Landau level orbits extend over characteristic lengths in the range 65–100 nm. These are comparable to, but do not exceed, the average spatial dot separation (≈ 100 nm), thus suggesting that in this sample Landau levels cannot form when the cyclotron orbit is larger than the average dot separation. The observation of the series of oscillations S2 in the $I(B_{\perp})$ for $V \geq 0.2$ V is likely to be related to the effect of screening of the disordered QW potential by the 2DEG which forms in the emitter accumulation layer when the applied bias is increased.²⁷ This screening effect may also enhance the recovery of the EI resonance in $I(V)$ induced by B_{\parallel} , shown in Fig. 2.

In conclusion, we have carried out magnetotunneling spectroscopy measurements on a RTD in which the active layer is a QW incorporating a layer of QD's at its center. These measurements indicate that the QD's affect strongly the potential in the QW on a characteristic length $l_d \approx 30$ nm, of the same order of the QD size and separation. As a result, the resonance in the $I(V)$ curve associated with the lowest QW subband is suppressed. However, when a strong magnetic field is applied in the plane of the QW, so that electrons tunnel from the emitter into QW state with a large component of in-plane k vector $k_{\parallel} > 2\pi/l_d$, the resonant peak in $I(V)$ is recovered. The states which electrons occupy at these large in-plane kinetic energies are extended bandlike states with well-defined momentum. Finally, magneto-oscillations in the tunnel current indicate the formation of Landau levels in the QW when the cyclotron orbit diameter is smaller than the average dot separation.

This work was supported by the Engineering and Physical Sciences Research Council (United Kingdom), the NANOMAT project of the EC Growth program Contract No. G5RD-CT-2001-0054, INTAS (Grants Nos. 00-0744 and 01-2362) and the Russian Foundation for Basic Research.

*Electronic address: fabio.pulizzi@nottingham.ac.uk

[†]Present address: Nanomaterials Laboratory, National Institute for Material Science, 1-2-1 Sengen, Tsukuba 305-0047, Japan.

¹D. Bimberg and M. Grundmann, *Quantum Dot Heterostructures* (Wiley, New York, 1999).

²H. Sakaki, G. Yusa, T. Someya, Y. Ohno, and T. Noda, *Appl. Phys. Lett.* **67**, 3444 (1995).

³E. Ribeiro, R.D. Jaggi, T. Heinzl, K. Ensslin, G. Medeiros-Ribeiro, and P.M. Petroff, *Phys. Rev. Lett.* **82**, 996 (1999).

⁴G.H. Kim, J.T. Nicholls, S.I. Khondaker, I. Farrer, and D.A. Ritchie, *Phys. Rev. B* **61**, 10 910 (2000).

⁵A.J. Shields, M.P. O'Sullivan, I. Farrer, D.A. Ritchie, K. Cooper,

C.L. Foden, and M. Pepper, *Appl. Phys. Lett.* **74**, 735 (1999).

⁶R.J.A. Hill, A. Patanè, P.C. Main, L. Eaves, B. Gustafson, M. Henini, S. Tarucha, and D.G. Austing, *Appl. Phys. Lett.* **79**, 3275 (2001).

⁷M. Narihiro, G. Yusa, Y. Nakamura, T. Noda, and H. Sakaki, *Appl. Phys. Lett.* **70**, 105 (1997).

⁸E.E. Vdovin, A. Levin, A. Patanè, L. Eaves, P. Main, Y.N. Khanin, Y.V. Dubrovskii, M. Henini, and G. Hill, *Science* **290**, 122 (2000).

⁹A. Patanè, R.J.A. Hill, L. Eaves, P.C. Main, M. Henini, M.L. Zambrano, A. Levin, N. Mori, C. Hamaguchi, Yu.V. Dubrovskii,

- E.E. Vdovin, D.G. Austing, S. Tarucha, and G. Hill, *Phys. Rev. B* **65**, 165308 (2002).
- ¹⁰G. Yusa and H. Sakaki, *Appl. Phys. Lett.* **70**, 345 (1997).
- ¹¹A. Schliemann, L. Worschech, S. Reitzenstein, S. Kaiser, and A. Forchel, *Appl. Phys. Lett.* **81**, 2115 (2002).
- ¹²K. Yoh, H. Kazama, Y. Kitashou, and T. Nakano, *Phys. Status Solidi B* **204**, 378 (1997).
- ¹³A. Polimeni, M. Henini, A. Patanè, L. Eaves, P.C. Main, and G. Hill, *Appl. Phys. Lett.* **73**, 1415 (1998).
- ¹⁴K.M. Groom, A.I. Tartakovskii, D.J. Mowbray, M.S. Skolnick, P.M. Smowton, M. Hopkinson, and G. Hill, *Appl. Phys. Lett.* **81**, 2002 (2002).
- ¹⁵J.-W. Sakai, T.M. Fromhold, P.H. Beton, L. Eaves, M. Henini, P.C. Main, F.W. Sheard, and G. Hill, *Phys. Rev. B* **48**, 5664 (1993).
- ¹⁶J. Wang, P.H. Beton, N. Mori, L. Eaves, H. Buhmann, L. Mansouri, P.C. Main, T.J. Foster, and M. Henini, *Phys. Rev. Lett.* **73**, 1146 (1994).
- ¹⁷I.E. Itskevich, T. Ihn, A. Thornton, M. Henini, T.J. Foster, P. Moriarty, A. Nogaret, P.H. Beton, L. Eaves, and P.C. Main, *Phys. Rev. B* **54**, 16 401 (1996).
- ¹⁸R.K. Hayden, D.K. Maude, L. Eaves, E.C. Valadares, M. Henini, F.W. Sheard, O.H. Hughes, J.C. Portal, and L. Cury, *Phys. Rev. Lett.* **66**, 1749 (1991).
- ¹⁹U. Gennser, V.P. Kesan, D.A. Syphers, T.P. Smith III, S.S. Iyer, and E.S. Yang, *Phys. Rev. Lett.* **67**, 3828 (1991).
- ²⁰T. Reker, H. Im, L.E. Bremme, H. Choi, Y. Chung, P.C. Klipstein, and H. Shtrikman, *Phys. Rev. Lett.* **88**, 056403 (2002).
- ²¹K. Takehana, F. Pulizzi, A. Patanè, M. Henini, P.C. Main, L. Eaves, D. Granados, and J.M. Garcia, *J. Cryst. Growth* **251**, 155 (2003).
- ²²A. Patanè, A. Polimeni, L. Eaves, P.C. Main, M. Henini, A.E. Belyaev, Y.V. Dubrovskii, P.N. Brounkov, E.E. Vdovin, Y.N. Khanin, and G. Hill, *Phys. Rev. B* **62**, 13 595 (2000).
- ²³T. Schmidt, R.J. Haug, V.I. Falko, K.v. Klitzing, A. Forster, and H. Luth, *Europhys. Lett.* **36**, 61 (1996).
- ²⁴M.L. Leadbeter, L. Eaves, P. Simmonds, G. Toombs, W. Sheard, P. Claxton, G. Hill, and M. Pate, *Solid State Electron* **31**, 707 (1988).
- ²⁵B.R. Snell *et al.*, *Phys. Rev. Lett.* **59**, 2806 (1987).
- ²⁶L. Eaves, G.A. Toombs, F.W. Sheard, C.A. Payling, M.L. Leadbeter, E.S. Alves, T.J. Foster, P.E. Simmonds, M. Henini, and O.H. Hughes, *Appl. Phys. Lett.* **52**, 212 (1988).
- ²⁷Y.V. Dubrovskii *et al.*, *Nanotechnology* **12**, 491 (2001).